Journal of Power Sources 247 (2014) 967–974

Contents lists available at ScienceDirect

Journal of Power Sources

journal homepage: www.elsevier.com/locate/jpowsour

Sulphonated polyether ether ketone diaphragms used in commercial scale alkaline water electrolysis

Jesus Otero [a], Javier Sese [a, b], Igor Michaus [c], Maria Santa Maria [d], Eugenio Guelbenzu [c], Silvia Irusta [a], Isabel Carrilero [c], Manuel Arruebo [a, *]

[a] Department of Chemical Engineering, Aragon Nanoscience Institute (INA), University of Zaragoza, C/ Poeta Mariano Esquillor S/N, 50018 Zaragoza, Spain
[b] Departamento de Física de la Materia Condensada, University of Zaragoza, 50009 Zaragoza, Spain
[c] Acciona Energía S.A., Avenida Ciudad de la Innovación, 5, E-31621 Sarriguren, Navarra, Spain
[d] Ingeteam Power Technology S.A., Avda. Ciudad de la Innovación, 13, E-31621 Sarriguren, Navarra, Spain

HIGHLIGHTS

- Sulphonated poly-ether-ether-ketone porous diaphragms were prepared by CIPS.
- SPEEK diaphragms were tested in a bipolar electrolyzer and in a 50 kW stack.
- Cell voltage and HTO were evaluated under normal and transient conditions.
- SPEEK diaphragms show lower cell voltage and HTO than commercial Zirfon®.
- SPEEK shows chemical stability after immersion in the electrolyte during 14 months.

GRAPHICAL ABSTRACT

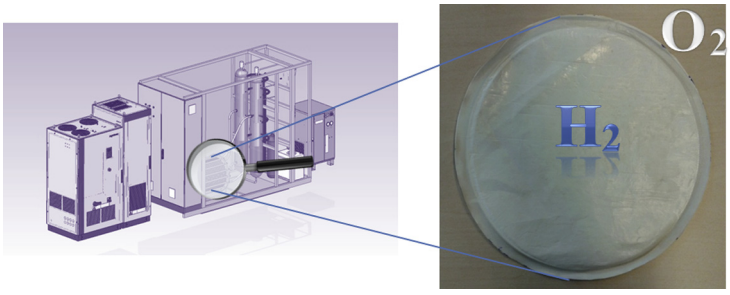

ARTICLE INFO

Article history:
Received 26 June 2013
Received in revised form
22 August 2013
Accepted 2 September 2013
Available online 24 September 2013

Keywords:
SPEEK
Alkaline electrolysis
Diaphragm
Zirfon
Stack
Poly-ether-ether-ketone

ABSTRACT

Sulphonated poly-ether-ether-ketone porous diaphragms were prepared by immersion precipitation using chemically induced phase separation to obtain a tight diaphragm skin layer and underneath finger-like bulk morphology. Different variables including sulphonation degree, diaphragm thickness, precipitation temperature and the presence of an inorganic filler were analyzed in order to evaluate the performance of the resulting diaphragms in water alkaline electrolysis using a bipolar electrolyzer and a commercial scale (50 kW) electrolyzer stack. Their performance was compared with a commercially available diaphragm in terms of cell voltage and oxygen purity (HTO) under normal operation conditions (10 bar, 80 °C) and under transient operation with up to 80 shutdown cycles (a total of 20 days in operation). Long term stability and operation reliability were assured for the SPEEK diaphragms showing lower cell voltage and HTO than the ones obtained with the commercial Zirfon® HTP 500 diaphragm.

1. Introduction

The global fuel cell and hydrogen energy market is projected to be worth over $180 billion in 2050 [1]. Global demand for hydrogen is anticipated to increase 4.1% annually through 2016 to reach 286

* Corresponding author. Tel.: +34 87655437; fax: +34 976761879.
E-mail address: arruebom@unizar.es (M. Arruebo).

0378-7753/$ – see front matter © 2013 Elsevier B.V. All rights reserved.
http://dx.doi.org/10.1016/j.jpowsour.2013.09.062

billion cubic metres [2]. To satisfy this great demand, mainly intended for ammonia production, petroleum refining and for chemical manufacturing, research is focused on improving existing hydrogen production technologies. Hydrogen can be produced by using thermochemical cycles or by direct electrolysis. Water electrolysis is one of the mature technologies which represent an emissions-free and highly efficient method for producing hydrogen with high purity particularly from renewable energies when small quantities and *in situ* production are required. Alkaline, proton exchange membrane and solid oxide are the three electrolytic technologies available today. Alkaline electrolyzers represent a well-established technology that is standard for large-scale electrolysis. To match the market supply/demand electricity balance, electricity is used to produce hydrogen which as an energy carrier can be stored (under pressure or liquefied) and transformed back into electricity by using a conventional fuel cell. The later can then operate with high efficiency even for low power ratings and can be used in transportation and in stationary power generation and their by-products are exclusively water and heat, making the overall process environmentally friendly. There are several processes and components of the overall hydrogen generation process, including its storage and its transformation into electricity which can be improved; one being the diaphragm of the alkaline electrolyzer.

The high capital expenses and the cost of electricity make still water electrolysis a non-competitive technology for mass hydrogen production and therefore, any improvement in the design, components and/or materials of the electrolyzer might represent a significant advancement towards being competitive in the commercial marketplace.

There are many approaches to lower the alkaline electrolyzers investment costs, for instance, by using cheaper construction materials [3]; and also to make them more efficient following different approaches such as by increasing the operational pressure of the system reducing the cost of compression before storage [4], by increasing the operation temperature to increase the electrolyte conductivity and to lower the polarization losses from the reactions in the electrodes [5] or even by increasing both pressure and temperature [6,7]. There are other alternatives to increase the efficiency of current alkaline electrolyzers including the development of more efficient electrodes to reduce mainly the cathodic overpotential [8,9], using zero-gap [10,11] or other energy-saving configurations [12], the usage of ionic activators [13], speeding up gas bubble disengagement from the electrolyte and from the surfaces of the diaphragm and electrodes by using high gravity [14], magnetic [15] or centrifugal forces [16], and the development of new diaphragm materials [17]. By increasing the temperature and the pressure the corrosion wear increases [18]. Even though higher electrolyte conductivities can be achieved at higher concentrations and temperatures [19,20] the trade-off is that corrosion also increases.

The effective electrical resistance of the separator is frequently as large as three to five times that of the electrolyte [21]. Therefore, there is considerable room for efficiency improvement in the design of new diaphragms while maintaining the required hydrogen to oxygen selectivity. The mission of the diaphragms is to separate the produced H_2 (cathode) and O_2 (anode) and avoid recombination. They should be ion-conductive (hydroxyl ions), hydrophilic, stable in 30 wt. % KOH at 80 °C and 10 bars (which are standard conditions for conventional alkaline water electrolysis), offer good mechanical stability and low electric resistance. Gas bubbles contained in the gas-supersaturated electrolyte should be excluded from the pores of the diaphragm in order to avoid excessive ohmic potential drop. In 1999 asbestos were forbidden to commercialize and to use in the EU [22] due to its demonstrated toxicity, so it could not be used as a construction material for diaphragms with the exception of existing electrolysis installations where the prohibition directive was derogated until 2015 [23]. PTFE and other hydrophobic polymers lack the necessary hydrophilic character and therefore ceramics (i.e., potassium titanates) or hydrophilic polymers are added to allow electrolyte pore filling [11]. Oxide-ceramic materials (i.e., YSZ, $NiTiO_3$/NiO, $BaTiO_3/ZrO_2/K_2Ti_6O_{13}$, supported on metallic nets (cermets) [24,25] have also been used although NiO and other nickel-based materials are as well substituted due to their toxicity. All nickel compounds except for metallic nickel have been considered a serious hazard to human health [26]. Current diaphragms are based on sulphonated polymers including poly(ethersulfone)'s [27], copolymers [28], perfluorinated sulfo-cationite membranes [29], and composite materials [30] where hydrophilic and brittle ceramics are embedded within a sulphonated polymer which acts as a binder and provides the required mechanical strength. Binder-free membranes composed yttria-stabilized zirconia interlocked fibres can also be used in alkaline electrolysis.

The aim of this work is to synthesize an anion conducting diaphragm as an electrode separator for alkaline water electrolysis. The target is to achieve greater energy efficiency and superior separation selectivity compared to commercially available ones. Results have generally been compared against the commercially available Zirfon® HTP 500.

2. Experimental

2.1. Materials and synthesis method

Poly-ether-ether-ketone (VESTA PEEK SP 2200, manufactured by LATI Industria Termoplastici S.p.A.), yttria stabilized zirconia (submicron powder 99.9%, Sigma–Aldrich) and sulphuric acid (96–98%) were used as received. PEEK is a semicrystalline thermoplastic polymer with an aromatic, non-fluorinated backbone, in which 1,4-disubstituted phenyl groups are separated by ether (–O–) and carbonyl (–CO–) linkages. PEEK can be sulphonated in solution following an electrophilic substitution reaction by using sulphuric acid to produce an ion-containing polymer bearing SO_3^- groups. In this way, PEEK powder was dried before sulphonation. This dry powder was added in H_2SO_4 under Ar atmosphere with stirring to reach a 4.7 wt. % concentration. Different sulphonation times (2, 5, 7 h) were used to obtain different sulphonation degrees (DS) (measured by RMN and elemental analysis) on the polymeric backbone. Diaphragm fabrication was carried out by immersion precipitation and chemically induced phase separation (CIPS), in which the polymer/solvent mixture is immersed in a non-solvent (water) at constant temperature and insolubility is induced. H_2SO_4 diffuses towards the aqueous phase whereas SPEEK insolubility is induced. Depending on the composition of the polymer solution/water mixture, phase separation can be initiated for this liquid–liquid phase, a crystallization process or a combination of both events. In doing so, the sulphonated solution was poured on a glass container and dragged to achieve the desired thickness with the aid of a doctor blade before water immersion. The casted film was then neutralized to stop sulphonation reaction of possible sulphuric acid retained into the diaphragm and finally dried (to constant weight) at room temperature. Membranes of 15.5 cm (bipolar cell) and 19 cm (stack) in diameter were prepared following this protocol. Their thicknesses were measured in 10 different points and averaged.

In some preparations, the commercial yttria stabilized submicrometric zirconia was used as inorganic filler to increase the hydrophilicity of the resulting diaphragms. In those cases a 5 wt. % of the filler was added on the polymeric solution prior to casting.

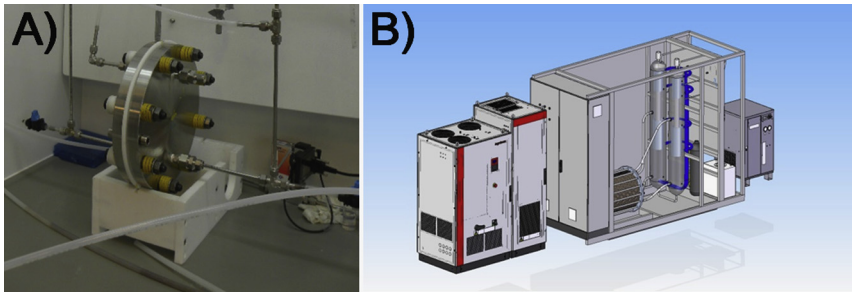

Fig. 1. Proprietary alkaline electrolyzers A) bipolar cell; B) bipolar stack including the hydrogen generation unit itself, the control panel and power rack, HTO monitoring, pressure and temperature sensors, H_2 purification system, separators, electrolyte reservoir and additional cooling system.

2.2. Electrolyzer installation

A proprietary design alkaline electrolyzer was used to evaluate the operational features of the different diaphragms operating at 80 °C, 10 bar and an electrical current density of 0.4 A cm^{-2} operating in the bipolar configuration. The cell stack uses the bipolar arrangement, where the cathode of one cell is at the same potential as the anode of the previous cell. Instead of connecting each cell electrically, only the cathode of the first cell and the anode of the last cell are connected to the power supply (Fig. 1). In the stack configuration (4 diaphragms), same electrical current density is used on a surface of 250 cm^2. The electrolyzers were equipped with two cast Ni mesh electrodes without the usage of additional catalysts. The diaphragm was placed in the middle of the electrolytic cell and separated from the electrodes by means of gas collectors which direct generated bubbles to the gas separators. The ratio of hydrogen to oxygen (HTO, H_2 concentration in the generated O_2 stream) is continuously analyzed by a gas sensor (Sensotran S.L., Spain) which is periodically calibrated using gas chromatography. A protective overvoltage was not applied at the electrolysis stack when the plants were in stand-by mode. In the electrolyzer, the OH^- ions migrate through the KOH (30 wt. %) electrolyte to reach the anode where the OH^- ions gain electrons producing H_2O and O_2. In the bipolar cell, this oxygen and the hydrogen generated from the water at the cathode side were separately evacuated through conical flasks used as gas–liquid separators. KOH electrolyte is fed from a storage tank to both the anode and cathode chambers. The stack itself is composed of 4 single cells connected in series using bipolar cell construction. Separating the individual cells from each other are metal plates, which act as conductors between the cells. Each plate serves as the anode for one cell and as the cathode for the neighbouring cell. For the experiments, both hydrogen and oxygen are exhausted to the atmosphere after measuring their volumetric flows and purities. Before testing, the diaphragms were saturated overnight in a KOH solution (30 wt.%) at room temperature.

2.3. Characterization techniques

An estimation of the wettability was possible using the bubble-point (BP) pressure test. This BP pressure is the pressure needed to blow air through a liquid-filled diaphragm. The top of the diaphragm was placed in contact with water which fills all the pores when the diaphragm is wetted. The bottom of the diaphragm is in contact with air and as the air pressure is gradually increased bubbles of air penetrate through the diaphragm at a certain pressure. The pressure corresponding to the first air bubble penetrating through the diaphragm is called the BP pressure. Therefore, the BP depends on the effective diameter of the largest pores.

The total porosity of the resulting diaphragms was evaluated in a mercury intrusion porosimeter (Micromeritics™ AutoPore IV).

Ageing effects on the as prepared diaphragms were evaluated by immersing samples of each diaphragm in Teflon lined autoclaves with KOH (30 wt. %) at 80 °C for different periods of time (up to 14 months) to evaluate their long term stability. After each sampling time (monthly), the samples were washed, dried and their weight loss was evaluated by mass balance.

In order to determine the sulphonation degree (SD) of SPEEK polymer, hydrogen nuclear magnetic resonance analysis (^{1}H NMR) was conducted using Bruker Avance 300 NMR Ultrashield spectrometer at a resonance frequency of 300 MHz for ^{1}H. For each analysis, approximately 3 wt. % polymer solution was prepared in deuterated dimethyl sulfoxide (DMSO-d_6) and tetramethylsilane was used as the internal standard.

An Inspect™ F high current FEG SEM (FEI Instruments) was used to characterize the structure and morphology of the resulting diaphragms. The cross section was observed by immersing the diaphragms in a liquid N_2 bath and creating a fracture. Samples were gold sputtered before observation.

Thermogravimetric analysis on the different polymeric and composite diaphragms was carried out using a TGA-DTA SDT 2960 from TA Instruments to evaluate the added amount of inorganic oxide filler (micro-ZrO_2). Differential Scanning Calorimetry (Mettler Toledo DSC822) was used to evaluate the glass transition temperatures of the polymers.

Fourier transform infrared (FTIR) spectroscopy of the polymeric diagrams was performed with a Bruker Vertex 70 FTIR spectrometer equipped with a DTGS detector and a Golden Gate diamond ATR accessory in order to analyze the stability of the chemical bonds of the polymeric backbone. Spectra were recorded by averaging 40 scans in the 4000–600 cm^{-1} wavenumber range at a resolution of 4 cm^{-1}. Data evaluation was carried out by using the OPUS software from Bruker Optics, Inc.

A sequential XRF spectrometer (Thermo Electron mod. ADVANT'XP) was used to carry out an elemental analysis on the polymeric diaphragms.

3. Results and discussion

3.1. Physico-chemical evaluation of the diaphragms

Fig. 2 shows the structure and morphology of the resulting SPEEK diaphragms after immersion precipitation. Their porosity depends on the phase separation kinetics, controlled in this work by polymer concentration and non-solvent temperature, the porosity of the resulting diaphragm could be modified. The diaphragm prepared by quenching the cast solution in a water bath a 60 °C consisted of a homogeneous top layer (skin) with nanometric pores in the skin and macropores with an open pore structure running perpendicular to it. Hence, this microcellular core structure is encased by the skin on one side (the one that first comes in contact with the water) and by the pore walls which fold over

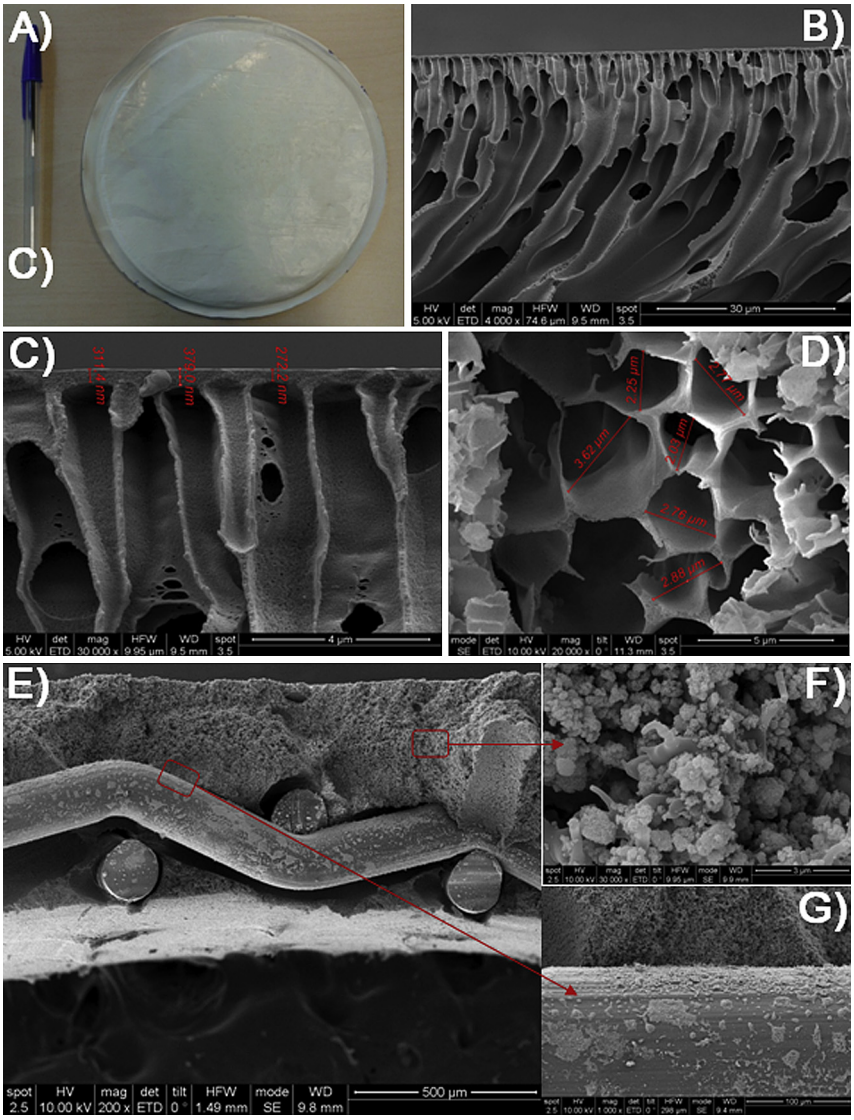

Fig. 2. Optical and SEM micrographs of the different diaphragms prepared by quenching the cast solution in a water bath at 60 °C. Synthesized SPEEK diaphragm (DS = 45.6%, 350 µm diaphragm thickness): A) general view, B and C) cross sections, D) top view close to the opposite side of the skin, and E–G) SEM micrographs of the cross-section of commercial Zirfon®.

themselves on the opposite side. Those pore walls represent a barrier against bubble clogging. This asymmetric diaphragm shows a very thin skin (200–400 nm) selective to gas bubbles (results not shown), overlaying a thick and highly porous (2–4 µm) sublayer which provides the diaphragm with the needed mechanical strength. Such a tight skin layer hinders gas bubbles from clogging the pores with the consequent increase in the electrical resistance and it also provides high capillary forces keeping the diaphragm wet and avoiding gas bubbles to penetrate it. During diaphragm formation as the solvent diffuses out of the top layer, the polymer concentration at that layer increases, resulting in a more compact skin layer compared with the open porosity of the layer below. The thickness of the skin could be modified depending on the temperature of the precipitation-water bath as shown later. Fig. 2 also shows the morphology of the Zirfon® diaphragm for comparison. Zirfon® contains 85 wt. % of a hydrophilic ZrO_2 powder with a high specific surface area to ensure an optimum wettability and 15 wt. % polysulfone which gives the material its mechanical strength [30]. The thickness of this organic-mineral diaphragm used as a reference was 500 µm. According to Vermeiren et al. [31] the absorption of water on the sub-micropores of Zirfon® is very fast and the bubble-point pressure is always higher than 0.1 MPa.

According to our observations, during SPEEK formation, the lower the temperature of the coagulation bath, the thicker the skin-layer obtained (Fig. 3). A thicker skin layer implies a greater resistance to mass transport and therefore a higher voltage is expected due to its greater resistance. The skin thicknesses were modified from ~2 µm, ~1 µm, 600–800 nm, to 200–400 nm when the precipitation bath temperature was set at 0, 20, 40 and 60 °C, respectively. Even though the thickness of the skin layer was affected by the precipitation-bath temperature, the overall thickness of the diaphragms was unaffected (Table 1) and they all showed a closed cell morphology with a narrow pore-size distribution. This elevated porosity allows for a fast migration of the hydroxyl ions through the porous diaphragm to the anode under the influence of the electrical field between both cathode and anode. Those hydroxyl ions discharge in the anode to generate oxygen and water. Therefore, the phase inversion technique allows controlling the thickness of the skin layer depending on the coagulation bath temperature and a lower skin thickness promotes a

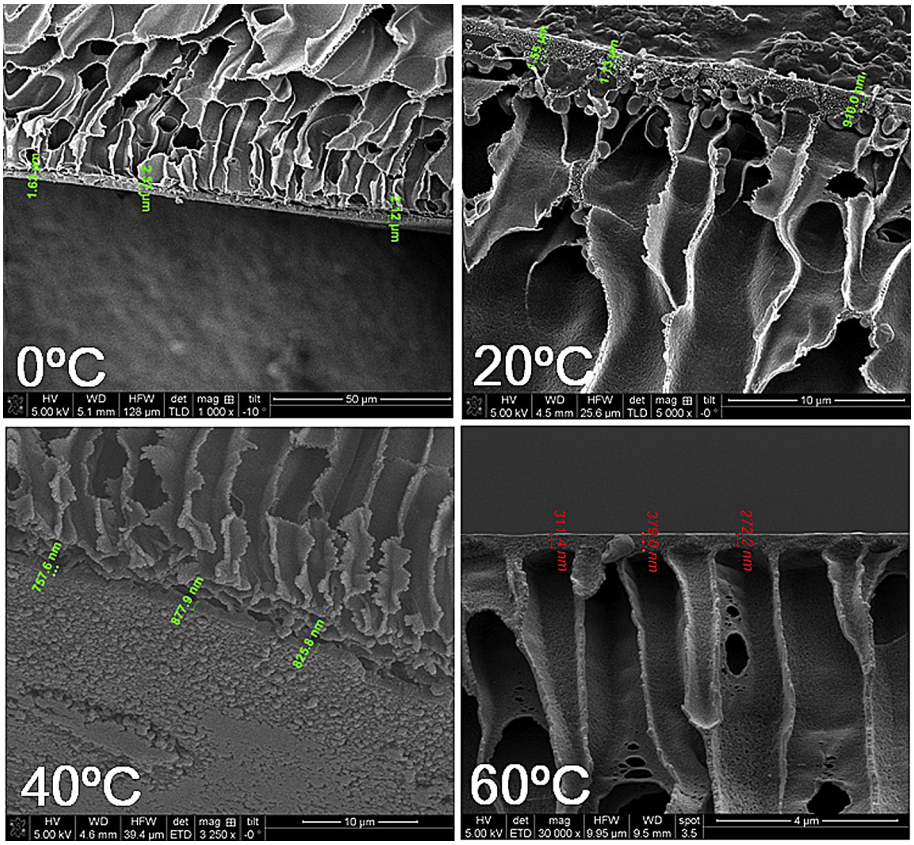

Fig. 3. SEM micrographs of different SPEEK diaphragms showing the different skin thicknesses depending on the temperature of the coagulation bath.

faster transport. Lower bath temperatures imply a higher cooling rate and the polymeric chains have less free movement before reaching the equilibrium leaving a more compact and thicker skin layer.

Mercury porosimetry for the resulting diaphragms revealed around 80% porosity (total void space within the porous diaphragm as a fraction of bulk volume) and a relatively narrow distribution of fine interchannel pores between 2 and 5 μm (median pore diameter in volume) which is in good agreement with the SEM observations.

FTIR spectra (Fig. 4) revealed the characteristic chemical bonds of SPEEK. The broad band observed at 3460 cm^{-1} for the SPEEK compared to pure PEEK is assigned to O–H vibrations from sulphonic acid groups interacting with molecular water [32]. Sulphonic groups have characteristic adsorption bands at 1250–1140 cm^{-1} (asymmetric SO_3 stretch) and 1070–1030 cm^{-1} (symmetric SO_3 stretch) and absorption bands for the ether groups at 1010–1120 cm^{-1} were also observable [33]. The C–S stretch bond at 710 cm^{-1} is also shown indicating that the sulphonation process was efficient. It has been reported [34] that the DS (calculated from NMR spectroscopy and from elemental analysis) correlates linearly with the ratio of the absorbances of the bands at 1470 and 1490 cm^{-1}. In our case, a strong positive linear relationship was observed with a linear correlation coefficient of 0.8 (results not shown). In ^1H NMR spectra, the determination of the presence of sulphonic acid groups in the polymer is based on the intensity signal at H_{13} [35]. When the sulphonic functional group is

Table 1
Comparative chart between Zirfon® used as reference and the novel SPEEK diaphragms showing % of increase (expressed as a positive percentage) or % of decrease (expressed as a negative percentage) of the cell voltage and HTO for the bipolar lab-scale electrolyzer depending on the different variables modified including sulphonation degree, diaphragm thickness and temperature of the precipitation bath. $N \geq 3$.

	Diaphragm	Outcome				
		DS (%)	Thickness (μm)	T_{Bath} (°C)	Cell voltage	HTO
	ZIRFON	–	500	–	2.476 ± 0.05 V	0.214 ± 0.03%
		DS (%)	Thickness (μm)	T_{Bath} (°C)	Variation of voltage	Variation of HTO
	SPEEK	40%	350	60	+1.8 ± 0.1%	−52.0 ± 21.8%
SPEEK	↓*DS*	↓ (37.6%)	350	60	+7.8 ± 1.7%	−14.5 ± 3.0%
	↓*Thick*	40%	↓ (184 ± 82)	60	−0.2 ± 6.3%	−17.5 ± 7.9%
	↓*Temp*	40%	350	20	+13.8 ± 2.7%	N/A
	↓*DS* − ↓*Thick*	↓ (31.5%)	↓ (163 ± 40)	60	+2.0 ± 5.7%	−60.3 ± 4.2%
	↓*DS* − ↓T_{Bath}	↓ (37.8%)	350	20	+27.4 ± 7.9%	N/A

Note: Example of the calculations to explain the results shown: The cell voltage obtained when using SPEEK was as an average 2.521 V. This value compared to the obtained for the reference Zirfon® (2.476 V) represents a 1.8% increase (represented with a positive sign) in the resulting cell voltage. The same SPEEK diaphragm showed up to a 52% reduction (represented with a negative sign) in the hydrogen content in the produced oxygen stream (HTO). While Zirfon® produced an HTO value of 0.214%, SPEEK yielded an average of 0.103%.

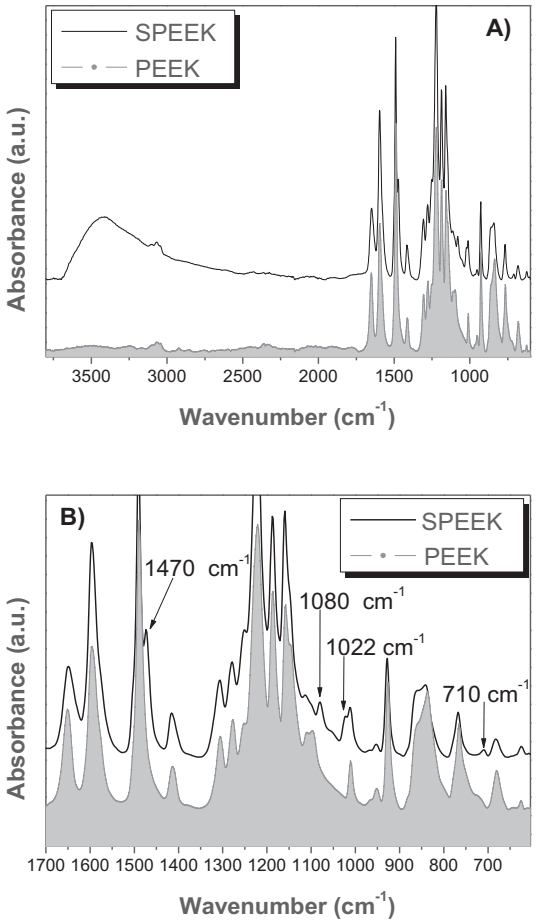

Fig. 4. FTIR spectrum of PEEK and SPEEK showing the characteristic sulphonic groups on the polymeric backbone. A) General survey; B) zoom of the area of interest.

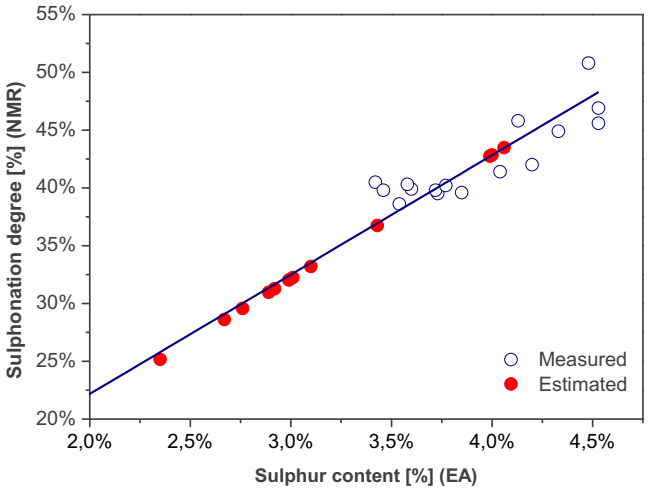

Fig. 5. Correlation of sulphonation degree (RMN) and sulphur content (EA) of regular diaphragms and the calculation of low-grade sulphonation diaphragms.

introduced to the aromatic ring, this type of proton tends to differentiate into three categories; H_{13} (the singlet at ~7.506 ppm), H_{14} (the doublet at ~7.203 ppm) and H_{15} (the doublet at ~7.12 ppm). The intensity of the signal at position H_{13} assures that the H_{13} content is equivalent to the SO_3 group content as a large down-field shift occurs for the hydrogen H_{13}. The difference in the DS of the resulting polymers can be estimated by evaluating the ratios between the peak area of the signal corresponding to the hydrogen atoms located next to the sulphonic acid groups (H_{13}) and the peak areas of the signals corresponding to the other aromatic hydrogen atoms (H_{14} and H_{15}) following the equation reported elsewhere [36]. When 7 h of sulphonation time was used a DS of 41.9 ± 3% was obtained. For shorter sulphonation times, 5 and 2 h, a DS of 35.3 ± 6% and 29.1 ± 3% respectively, were obtained; those values were calculated by the correlation of sulphur content (elemental analysis) with DS (NMR) data of regular diaphragms due to the impossibility of using NMR owing to the insolubility of those diaphragms with low-grade of sulphonation in DMSO-d_6 (Fig. 5). The DS did not affect the thickness of the resulting skin layer when using the same precipitation-bath temperature. A hydrophilic character is induced in the PEEK after sulphonation; however the chemical resistance to alkalis of the resulting film can be reduced with increasing sulphonation owing to the reduction of PEEK crystallinity. For that reason we studied the long term stability of the resulting diaphragms with different DS. Those long term stability studies in the ageing autoclaves indicated that the weight loss of SPEEK diaphragms (350 μm thick) was below a 2 wt. % after 14 months of immersion in the electrolyte at 80 °C. Thinner SPEEK diaphragms (160 μm) showed a weigh loss of 3.3 wt. % for the same period of time. FTIR analysis was also carried out on those aged diaphragms revealing an initial decrease in the intensity of the ether groups (1010–1120 cm^{-1}) after a few hours of immersion in the electrolyte, then remaining constant during the following 14 months. This is an indication that a partial chemical attack occurs after immersing the SPEEK diaphragm in the electrolyte, although the chemical properties remain unaltered during the period of time studied (14 months) and no brittleness is detected. A lower decrease for that initial ether-group loss was measured for the YSZ filled diaphragms compared to the un-filled SPEEK ones.

The glass transition temperature of the parent PEEK measured by DSC was 148 °C in agreement with the manufacturer specifications. The sulphonation increased that transition temperature to 155–165 °C depending on the sulphonation degree, in agreement with results previously reported [32], indicating that the chemical structure of repeating units of the polymer, its bulkiness and the interaction of chains was modified in this thermostable polymer. This increase is a consequence of the hydrogen bonding between sulphonic acid groups that suppresses the segmental motion of the chains [37].

Bubble-point tests together with the evaluation of the nominal filtration rate with the aid of commercially available latex micro (1–3 μm) and nanoparticles (50–200 nm) revealed a bubble point pressure of 3 bar and a nominal filtration rate <1 μm ($\Delta P = 1$ bar). Particles of 500 nm in diameter permeate through the SPEEK diaphragm but 1 μm particles did not. This cut-off indicates that gas bubbles with sizes above 1 μm would be excluded from the diaphragm.

3.2. Performance in the electrolytic cell (bipolar cell and stack)

A representative cell potential variation over time in the bipolar cell for different SPEEK diaphragms compared to commercial Zirfon® is depicted in Fig. 6. Depending on the SPEEK-diaphragm thickness the cell voltage can be reduced. In general, the thinner the diaphragm thickness, the lower the cell potential, due to its lower resistance. Table 1 shows cell voltages together with HTOs for the different diaphragms ($N \geq 3$ for each variable studied) prepared in this work shown as % of improvement or impairment with respect to the Zirfon® used as a reference. SPEEK is superior to the Zirfon® tested in terms of cell voltage and O_2/H_2 selectivity. This oxygen presence in the hydrogen stream can be caused by the solubility of the gases in the electrolyte (which will increase with

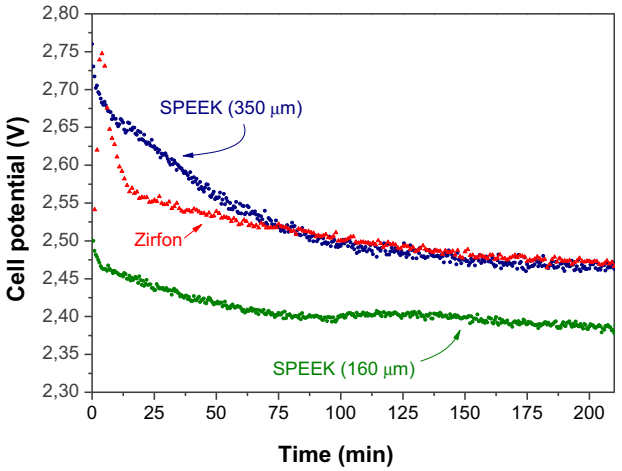

Fig. 6. Cell potential over time for two SPEEK diaphragms of different thickness. Zirfon® behaviour is shown as a reference. T_a = 80 °C; 10 bar, 0.4 A cm^{-2}. The DS of the SPEEK diagrams is 39.5% (350 μm) and 40% (160 μm).

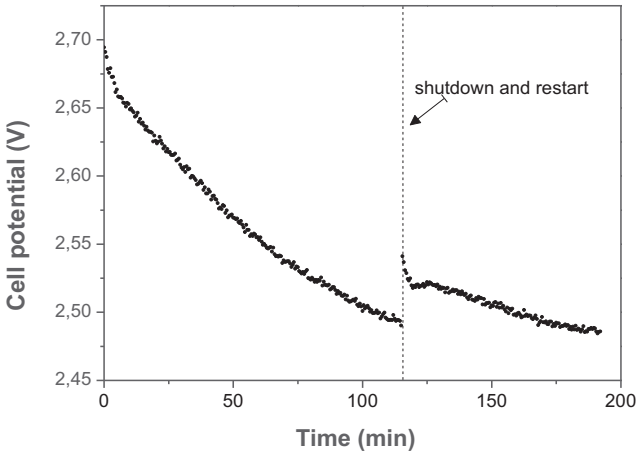

Fig. 7. Cell potential over time under transient operation for a SPEEK diaphragm (350 μm, DS = 40%) with a shutdown cycle T_a = 80 °C; 10 bar, 0.4 A cm^{-2}.

pressure) and consequently in the gas separators and by the presence of non-selective defects in the diaphragm. Not only low electric power consumption but also the quality of the produced hydrogen is an important factor when evaluating the performance of the resulting diaphragms and a higher selectivity will render a hydrogen stream of higher purity. It is important to point out that no shrinkage effects were observed in all the SPEEK diaphragms tested after operation. A lower DS increases the diaphragm hydrophobicity by decreasing the number of protonated sites (−SO_3H) and therefore the cell voltage increases, probably due to the accumulation of gas bubbles in the diaphragm surface. However, a lower DS increases the chemical stability of the resulting diaphragm. As we mentioned before, a lower temperature in the precipitation bath induces a larger skin thickness and consequently a greater resistance. A trade-off can be reached by simultaneously reducing the diaphragm thickness and the DS. By doing so, a thinner diaphragm can overcome the higher cell potential obtained with diaphragms with a lower DS highlighting the versatility of SPEEK as building material for diaphragms in alkaline electrolysis. "A H_2 production of 0.6 Nm^3/day was obtained when using the lab-scale bipolar electrolyzer and this production depended exclusively on the current density applied. This production was the same irrespectively of the diaphragm used (Zirfon® or SPEEK) when working at the same current density; however, the necessary cell voltage strongly depended on the diaphragm used as we describe in Table 1".

By including zirconia as filler (5 wt. %) in the diaphragms the cell voltage obtained remained statistically unaltered (results not shown) with respect to the same unfilled diaphragm indicating that the wettability conditions of the unfilled SPEEK are sufficient for the desired application. The filler was introduced with the aim of reducing the conduction losses when low humidity contents are noticeable in a diaphragm. Probably larger amounts of the hydrophilic filler would be needed to observe a measurable effect; however the purpose of the synthesis was to obtain a functional diaphragm as simple as possible and without the need of a secondary additive. Yttria stabilized submicrometric zirconia shows high ionic conductivity and electrochemical stability which facilitates its use in electrolysis. By increasing the zirconia loading in the composites a larger water uptake was expected with its corresponding enhancement in its mechanical properties. In our case a 5 wt. % loading did not render statistically significant improvements over the unmodified SPEEK indicating the absence of diffusion limitation constrains for the electrolyte to fill the diaphragm pores in.

The electrolyzers can run in non-stationary operation because of the highly variable load produced by the typical renewable energy sources. Therefore, the electrolyzer should respond to load change gradients in the order of minutes [38]. Also, there is a need of energy in remote or isolated locations based on hydrogen technologies integrated with renewable energy sources, in non-grid-connected applications, for which alkaline electrolyzers can operate when the energy is needed to produce hydrogen. In those scenarios the produced hydrogen is separately stored and converted back into electricity by using a fuel cell operating very often in an intermittent status. Transient operation with a shutdown cycle is shown in Fig. 7 where it can be seen that in less than 40 min after the shutdown the electrolyzer reaches the same values. The stack configuration showed larger differences between both SPEEK and Zirfon® compared to the variability observed when using the bipolar cell (Fig. 8). Also, the response time to reach a steady value is shorter in the stack configuration compared to the bipolar one. Due to the reduced thickness used in the stack configuration (4 diaphragms 211 ± 50 μm thick) the cell voltage was reduced by 18% compared to the standard Zirfon® tested which would imply a large energy saving for the water electrolysis industry. Also it is important to point out that under those conditions tested on a

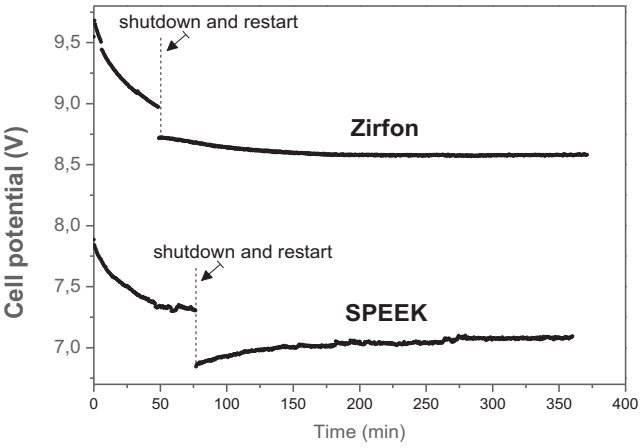

Fig. 8. Cell potential over time in the stack (4 diaphragms in bipolar arrangement, where the cathode of one cell is at the same potential as the anode of the previous cell. SPEEK thickness 211 ± 50 μm and DS = 40.3 ± 0.8%) under transient operation with a shutdown cycle T_a = 80 °C; 10 bar, 0.4 A cm^{-2}.

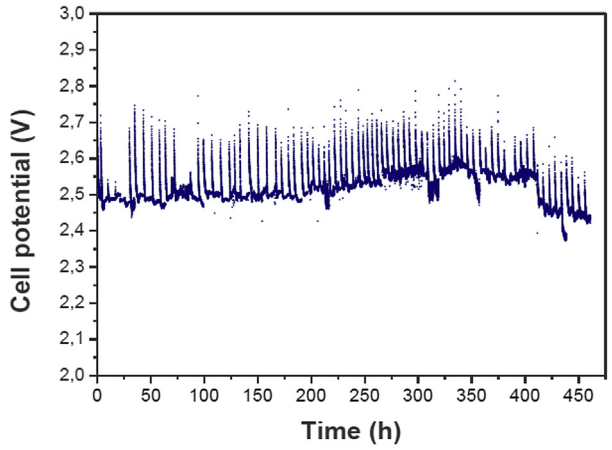

Fig. 9. Cell potential over time (bipolar cell, SPEEK thickness 350 μm, DS = 40%) under transient operation with up to 80 shutdown cycles (a total of 20 days in operation). $T\underline{a}$ = 80 °C; 10 bar, 0.4 A cm^{-2}.

commercial scale electrolyzer, the elevated pressure (10 bar) would facilitate the storage of the produced hydrogen.

In conventional alkaline electrolysis a protection current during operational shut-down times is necessary to avoid shunt currents; however in our case we operated in the most adverse scenario without protective current in order to evaluate the response and reliability of the SPEEK diaphragms under those transient conditions. In this way, cell potential over time (bipolar cell, SPEEK thickness 350 μm) under transient operation with up to 80 shutdown cycles (a total of 20 days in operation) is shown in Fig. 9. As it is demonstrated, the SPEEK diaphragm shows high reliability with an average cell potential for those 20 days of 2.51 ± 0.39 V (discarding the initial data points after the burst restart of each day) indicating that they could be potentially used to store intermittent renewable energy from an unsteady resource such as wind power. The voltage changes are considered to be caused by the change in the electrodes condition, not due to the diaphragm itself. Those current spikes noted immediately after the application of power to the stack following the interruption event is characteristic of electrochemical reactions and are attributed to the shedding of an electrode oxide layer that becomes unstable at low potentials [39]. After those 20 days of operation the diaphragm did not undergo any variation on its physic-chemical properties.

4. Conclusions

SPEEK membranes have been widely used as a polyelectrolyte material for proton exchange membranes (PEM) in fuel cells; however, this is the first time that those membranes have been used in alkaline water electrolysis showing a superior performance in terms of gas purity and cell voltage compared to commercial Zirfon® HTP 500 diaphragms. SPEEK shows chemical stability after immersion in the electrolyte (KOH 30 wt.%) at 80 °C during 14 months indicating its excellent thermal, oxidative and hydrolytic stability. By reducing the diaphragm thickness without compromising the chemical stability of those SPEEK diaphragms over time, it is possible to achieve an 18% reduction in the cell voltage operating in a 50 kW electrolyser unit with stack configuration at a current density of 400 mA cm^{-2} and operation pressure of 10 bar. The low HTO values obtained with the SPEEK diaphragms indicate that intermixing between the oxygen-saturate anolyte and the hydrogen-saturated catholyte is reduced. Even under transient operation with up to 80 shutdown cycles (a total of 20 days in operation) the diaphragm showed high voltage stability indicating its potential application in remote locations where interruptions are common or in off-grid applications. Rapid cycling without protection current accelerates degradation; however in our case the produced diaphragms show high stability over time with high efficiency. In summary, safety and reliability can be achieved using SPEEK-based porous diaphragms used in advanced alkaline electrolysis due to the low internal ohmic resistance that this polymer offers and its high separation selectivity achieved.

Acknowledgements

We gratefully acknowledge Acciona Energy S.A. and Ingeteam Power Technology S.A. for their financial support within the INNPACTO DESPHEGA (Ministry of Science and Innovation, Spain) under grant IPT-120000-2010-010.

References

[1] (PATH), P.f.A.t.T.t.H.Annual Report on World Progress in Hydrogen, 2011–2012, 2011, 2012. Available from: http://www.hpath.org/PATH%20Annual%20Report%20Press%20Release_FINAL.pdf
[2] G. Freedonia, World Hydrogen to 2016, 2012.
[3] D. Marcelo, A. Dell'Era, Int. J. Hydrogen Energy 33 (12) (2008) 3041–3044.
[4] M. Hammoudi, et al., Int. J. Hydrogen Energy 37 (19) (2012) 13895–13913.
[5] A. Hauch, et al., J. Mater. Chem. 18 (20) (2008) 2331–2340.
[6] F. Allebrod, C. Chatzichristodoulou, M.B. Mogensen, J. Power Sources 229 (0) (2013) 22–31.
[7] J.C. Ganley, Int. J. Hydrogen Energy 34 (9) (2009) 3604–3611.
[8] D.L. Stojić, et al., Int. J. Hydrogen Energy 30 (1) (2005) 21–28.
[9] R. Solmaz, A. Döner, G. Karda&scedil, Int. J. Hydrogen Energy 34 (5) (2009) 2089–2094.
[10] S. Marini, et al., Electrochim. Acta 82 (0) (2012) 384–391.
[11] D. Pletcher, X. Li, Int. J. Hydrogen Energy 36 (23) (2011) 15089–15104.
[12] H. Zhang, et al., Int. J. Electrochem. Sci. 6 (2011) 2566–2580.
[13] V.M. Nikolic, et al., Int. J. Hydrogen Energy 35 (22) (2010) 12369–12373.
[14] M. Wang, Z. Wang, Z. Guo, Int. J. Hydrogen Energy 35 (8) (2010) 3198–3205.
[15] T. Iida, H. Matsushima, Y. Fukunaka, J. Electrochem. Soc. 154 (8) (2007) E112–E115.
[16] H. Cheng, K. Scott, C. Ramshaw, J. Electrochem. Soc. 149 (11) (2002) D172–D177.
[17] C.-Y. Hung, et al., J. Membr. Sci. 389 (0) (2012) 197–204.
[18] C. Bailleux, Int. J. Hydrogen Energy 6 (5) (1981) 461–471.
[19] F. Allebrod, et al., Int. J. Hydrogen Energy 37 (21) (2012) 16505–16514.
[20] M.N. Manage, et al., Int. J. Hydrogen Energy 36 (10) (2011) 5782–5796.
[21] D.J. Pickett (Ed.), Electrochemical Reactor Design, Elsevier, Amsterdam, 1979.
[22] 1999/77/EC., U.D.Asbestos Ban, 1999
[23] The European Commission Decides to Prolong the Use of Asbestos in Certain Sectors, The European Trade Union Institute, April 12, 2013.
[24] H. Wendt, H. Hofmann, V. Plzak, Int. J. Hydrogen Energy 9 (4) (1984) 297–302.
[25] H. Wendt, H. Hofmann, Int. J. Hydrogen Energy 10 (6) (1985) 375–381.
[26] E. Denkhaus, K. Salnikow, Crit. Rev. Oncol./Hematol. 42 (1) (2002) 35–56.
[27] J. Kerres, et al., Desalination 104 (1–2) (1996) 47–57.
[28] S. Ravichandran, et al., Electrochem. Soc. 33 (27) (2011) 157–166.
[29] A.N. Ponomarev, Y.L. Moskvin, S.D. Babenko, Russ. J. Electrochem. 43 (3) (2007) 273–278.
[30] P. Vermeiren, et al., Int. J. Hydrogen Energy 23 (5) (1998) 321–324.
[31] P. Vermeiren, et al., Int. J. Hydrogen Energy 34 (23) (2009) 9305–9315.
[32] P. Xing, et al., J. Membr. Sci. 229 (1–2) (2004) 95–106.
[33] G. Infrared Characteristic Group Frequencies, Socrates John Wiley & Sons, New York, 1980, pp. 111–116.
[34] R.T.S. Muthu Lakshmi, V. Choudhary, I.K. Varma, J. Mater. Sci. 40 (3) (2005) 629–636.
[35] S.S. Mohtar, A.F. Ismail, T. Matsuura, J. Membr. Sci. 371 (1–2) (2011) 10–19.
[36] W.J. Lau, A.F. Ismail, J. Membr. Sci. 334 (1–2) (2009) 30–42.
[37] S. Swier, et al., Polym. Eng. Sci. 45 (8) (2005) 1081–1091.
[38] C. Ziems, D. Tannert, H.J. Krautz, Energy Procedia 29 (0) (2012) 744–753.
[39] A. Bergen, et al., Int. J. Hydrogen Energy 34 (1) (2009) 64–70.